scientific reports

Check for updates

OPEN

Deciphering the molecular impact of *ALDH5A1* missense variants in succinic semialdehyde dehydrogenase deficiency through combined in vitro and in silico approaches

Giulia Spagnoli[1,11], Samuele Cesaro[1,9,11], Cristian Andres Carmona Carmona[1,10], Davide Tonduti[2,3], Fabio Bruschi[2,3], Valentina Belacchi[4], Stefania Paganini[5], Itay Tokatly-Latzer[6,7], Phillip L. Pearl[6], Giovanni Bisello[1], Miroslava Didiasova[8], Ritva Tikkanen[8] & Mariarita Bertoldi[1]✉

Succinic semialdehyde dehydrogenase is a key enzyme involved in the catabolism of g-aminobutyric acid. Biallelic variants in the *ALDH5A1* gene cause a rare monogenic neurometabolic disorder, SSADH deficiency, characterized by a total or partial enzyme loss-of-function. Patients present symptoms from infancy on and mainly show developmental delay and intellectual disabilities, with seizures and/or autistic spectrum disorders as the main distinctive traits associated with the severe forms of the disorder. A valuable instrument to interpret variant function is provided by bioinformatic tools that are based on evolutionary and structural data. However, the results need to be complemented by other experimental approaches to dissect the molecular basis for the defect and be supportive of the clinical phenotype of patients. Here, we validate a bioinformatic prediction of loss-of-function using two recombinant enzyme variants and/or transient transfection in a *ALDH5A1* knockout HEK-293T cell model. These SSADH protein variants are synthesized by two functionally hemizygous SSADH deficiency patients. The known loss-of-function p.Gly176Arg variant was predicted by bioinformatic analyses to affect oligomerization. Indeed, we demonstrate that the variant acquires a tetrameric altered structure, possibly responsible for the loss-of-function. The pathogenicity of the new p.Pro234Ser variant is mainly due to its failure to reach the mature form, possibly due to its intrinsic instability rather than a defect in the maturation apparatus, thus preventing a correct folding process. Altogether, we provide evidence that combining recombinant protein studies with structural predictions can offer valuable insights into loss-of-function, which is essential for precision therapy.

Keywords Succinic semialdehyde dehydrogenase deficiency, Variants, Genotype-phenotype correlation, Spectroscopic and kinetic analyses, Knockout HEK-293T cell model

[1]Department of Neuroscience, Biomedicine and Movement Sciences, University of Verona, Strada Le Grazie, 8, 37134 Verona, Italy. [2]Child Neurology Unit, Vittore Buzzi Children's Hospital, 20154 Milan, Italy. [3]Department of Biomedical and Clinical Sciences, University of Milan, 20157 Milan, Italy. [4]Radiology Unit, IRCCS, Azienda Ospedaliera Universitaria di Bologna, 40138 Bologna, Italy. [5]Medical Genetics Laboratory, Clinical Pathology Foundation IRCCS Ca' Granda Ospedale Maggiore Policlinico, 20157 Milan, Italy. [6]Department of Neurology, Boston Children's Hospital, Harvard Medical School, 300 Longwood Ave, Boston, MA 02115, USA. [7]Gray School of Medicine, Gray Faculty of Medical and Health Sciences, Tel- Aviv University, Tel Aviv, Israel. [8]Institute of Biochemistry, Medical Faculty, University of Giessen, Friedrichstrasse 24, 35390 Giessen, Germany. [9]Present address: Center for Pediatric and Adolescent Medicine, Division of Pediatric Neurology and Metabolic Medicine, University Hospital Heidelberg, Heidelberg, Germany. [10]Present address: Biology Department, University of Padova, Padova, Italy. [11]Giulia Spagnoli and Samuele Cesaro: co-first authors ✉email: mita.bertoldi@univr.it

Succinic semialdehyde dehydrogenase (SSADH, E.C. 1.2.1.24) is a key mitochondrial enzyme involved in the catabolism of γ-hydroxybutyric acid (GABA). It catalyzes the NAD^+-dependent oxidation of the GABA-derived product of transamination, succinic semialdehyde (SSA), into succinic acid, an essential intermediate of the citric acid cycle. It thus plays a fundamental role in mitochondrial function, linking the modulation of succinic acid levels to the catabolism of glutamate (Fig. 1).

A functional defect in SSADH leads to the accumulation of both GABA and γ-hydroxybutyrate (GHB), a known toxic compound, with consequences for neurometabolic responses and neurotransmission.

SSADH deficiency (OMIM: #271980)[1,2] is a rare monogenic recessive neurometabolic disease (prevalence of 1:460,000[3]) caused by variants in the *ALDH5A1* gene (6p22.3, GRCh38.p13:24,494,969–24,537,207), resulting in partial or total enzyme loss-of-function[4,5]. Patients reveal symptoms from infancy on and mainly show developmental delay and intellectual disabilities, with seizures and/or autistic spectrum disorders as the main distinctive traits associated with the severe forms of the disorder[6–10]. The metabolic hallmarks of SSADH deficiency are the presence of high levels of GHB in the urine, blood, and/or cerebrospinal fluid (CSF)[2,4] and decreased SSADH activity in lymphocytes[11]. Diagnosis is confirmed by sequencing the *ALDH5A1* gene to identify biallelic variants. The treatment is primarily palliative or symptomatic, as recently reported in published guidelines[12], with no curative therapy available.

About 2800 *ALDH5A1* variants are recorded in GnomAD 4.1.0 (https://gnomad.broadinstitute.org/) (accessed on 12th December 2025), while ClinVar (https://www.ncbi.nlm.nih.gov/clinvar/) lists 740 variants (accessed on 12th December 2025), 49% of them recorded as missense, identified in about 500 patients reported in the literature[4]. Several pathogenic variants have been expressed in vitro in HEK-293T cells to measure their activity, as pioneered by Gibson and collaborators[13,14] (and references therein), as well as by recent reports concerning new variants[15–18].

Since the causative agent of the disease is the SSADH protein, which is either absent (due to splicing or deletion/insertion variants) or modified by single amino acid substitutions (missense variants), a more thorough understanding of its structural features, responsible for its function, is necessary. SSADH is a tetramer composed of four identical subunits arranged in a dimer of dimers assembly[19], in analogy to other members of the aldehyde dehydrogenase family. Each monomer contains 535 amino acids, partitioned into a mitochondrial targeting sequence (MTS, amino acids 1–47), a NAD^+-binding domain (amino acids 48–173, 196–307 and 509–524), a catalytic domain (amino acids 308–508) and an oligomerization domain (amino acids 174–195 and 525–535). From the position and type of chemical nature of the amino acid substitutions, the possible impact of some missense variants associated with SSADH deficiency has been suggested[19,20]. A recent kinetic study, coupled with structural information, laid the foundation for understanding the molecular impact on kinetic performance[21]. In this context, the typical employed method involves evaluating kinetic performance for each individual allelic variant. However, this strategy does not account for patients' genotypes and the related possibilities of combination of expressed polypeptide chains, an issue that must be understood to address the functional effects.

Such an approach has already been employed in an investigation focused on genotype-to-phenotype comprehension which allowed for the association of the worst and mildest SSADH deficiency clinical phenotypes[22] with specific combinations of SSADH tetrameric protein variants[23]. Notably, this predictive approach was entirely carried out through a bioinformatic evaluation of the impact of amino acid substitutions on the crystal structure, combined with outputs obtained from available in silico computational tools, which are based on evolutionary origin. Although meaningful for the first and fourth quartiles of the clinical severity score[22], the predictions require refinement for the other phenotypes and validation.

From this rationale, we cloned, expressed and purified two variants (p.Gly176Arg and p.Pro234Ser) and characterized them to understand the molecular basis for their defective catalysis, as already reported for other SSADH deficiency variants[24]. Indeed, p.Gly176Arg has already been reported in some patients both in homozygosis[25] and in compound heterozygosis with a null allele (hemizygosis)[23] or with another missense variant[13]. In the first two conditions, patients can synthesize one type of polypeptide chain that theoretically can lead to the formation of the p.Gly176Arg homotetramer (with the same substitution in all four subunits), whereas in the third case there is a constellation of possible SSADH tetramers with different subunit combinations[26]. The substitution of Gly-to-Arg was predicted to affect oligomerization as Gly176 is part of a stretch involved in subunit interactions[19,23] and was reported to result in a loss-of-function following expression in HEK-293 T cells[13]. The second variant (p.Pro234Ser) is new and has been identified in an Italian patient with no known functional or clinical data.

Altogether, we provide here evidence that combining recombinant protein studies and cell expression studies with structural predictions can offer valuable insights into loss-of-function, which is essential for precision therapy approaches.



Fig. 1. Effects of SSADH misfunctioning in its metabolic pathway. Graphical representation of altered glutamate metabolism in SSADH deficiency. Abbreviations: Glu, Glutamate; GAD, glutamate decarboxylase; GABA-T, GABA transaminase; SSAR, SSA reductase (AKR7A2); SA, succinic acid.

Materials and methods

Materials

Succinic semialdehyde (SSA), NAD^+, β-mercaptoethanol (BME), isopropyl-β-d-thiogalactopyranoside (IPTG), phenylmethylsulfonylfluoride (PMSF), and SigmaFast inhibitor cocktail were purchased from Merck (Darmstadt, Germany). Anti-SSADH and anti-His-tag antibodies were from Santa Cruz Biotechnology (Dallas, TX). All other chemicals were of the highest purity available.

Patients clinical data

All procedures were in accordance with the 1964 Helsinki declaration and its later amendments or comparable ethical standards. Written informed consent for this work was obtained from the patients' parents or legal caregivers. We confirm that we have read the Journal's position on issues involved in ethical publication and affirm that this work is consistent with those guidelines. The Succinic Semialdehyde Dehydrogenase (SSADH) Deficiency Natural History Study (NHS) is approved by the Boston Children's Hospital Institutional Review Board (#P00029917). All participants in the SSADH Deficiency NHS reviewed and signed an informed consent form.

Computational analysis: effects of in silico mutagenesis and Alpha Fold structural models

The human SSADH crystal structure (PDB 2W8O) (both the monomer and the tetramer) was superimposed with a structure obtained by in silico mutagenesis of the selected residues by the software PyMOL (Version 2.2.3, Schrödinger, Limited Liability Company; New York, NY, USA). The volume surrounding the residues Gly176 and Pro234 and their pathogenic variants was evaluated (sphere of 5 Å radius) focusing on the physical–chemical alterations in the protein structure.

Structural models of the p.Gly176Arg and p.Pro234Ser variants were generated using AlphaFold and superimposed onto the wild-type (WT) tetrameric structure for comparative analysis[27]. The effects of the variants on protein stability were independently evaluated using FoldX (five independent BuildModel runs)[28], DynaMut2[29], and DUET[30]. For FoldX calculations, the mutations were introduced simultaneously in all four subunits of the tetrameric assembly, whereas DynaMut2 and DUET analyses were performed using their standard prediction workflows.

Cloning, expression, and purification of WT and variant SSADH proteins in *E. coli*

For bacterial production of recombinant WT, p.Gly176Arg, and p.Pro234Ser/Ala variants, we used the procedure already reported[21,24] (Table S1 reports the primers for mutagenesis). Plasmid DNA (pET-15b) was obtained by propagation in *E. coli* DH5-α strain, and subsequently purified with QIAprep® spin miniprep kit (QIAGEN, Inc.).

Transient expression of WT and p.Ser234Pro in knockout (KO) HEK-293 T cells

For mammalian cell expression, human embryonic kidney cells (HEK-293T) (Invitrogen) and already reported HEK-293T Flp-In™-293 cells (Thermo Fischer Scientific) *ALDH5A1*-KO cells[24] were cultured at 5% CO_2 and 37°C in DMEM-GlutaMAX (Gibco, Thermo Fisher Scientific, Inc., REF 10569010), which was supplemented with 10% Fetal Bovine Serum (FBS), 1% Penicillin/Streptomycin. Cell detachment was performed by trypsinization with Trypsin–EDTA (Gibco, Thermo Fisher Scientific, Inc.). The vector pcDNA^{TM}4.1/TO carries the codon optimised version of *ALDH5A1* WT and p.Pro234Ser variant (Table S1) without MTS. All the plasmids employed in this study were validated by Sanger sequencing method (performed by Eurofins Genomics Europe Shared Services GmbH) to verify the accuracy of the construct for the entire Open Reading Frame (ORF). The quantification of all the genetic material was carried out in a NanoQuant Plate by the means of an Infinite 200 Pro Tecan plate reader (DKSH Holding Ltd).

Transient expression studies were conducted by seeding 3×10^5 cells onto 6-well tissue culture plates, followed, after 24 h, by the addition of the transfection mixture containing 1 µg of pcDNA^{TM}4.1/TO and Lipofectamine 3000 Transfection reagent (Themo Fisher Scientific, Inc.) according to the manufacturer's protocol. After 48 h, cells were incubated for 10 min on ice with RIPA lysis buffer and 1 × Complete protease inhibitor cocktail (F. Hoffmann-La Roche Ltd, REF 11697498001), and they were subsequently harvested by scraping. The cell suspension was then centrifuged for 10 min at 4°C, the supernatant and the pellet were collected for evaluating the expression, and the protein concentration was determined by Bradford assay (Bio-Rad DC Protein Assay 5000112, Hercules, US) in an Infinite 200 Pro Tecan plate reader (DKSH Holding Ltd.).

Mitochondrial isolation

HEK-293 T and HEK-293 T-KO cells were seeded at 2×10^6 and transiently transfected, after 24 h, with pcDNA^{TM}4.1/TO vector encoding for either WT or p.Pro234Ser SSADH, as described above. After 48 h, cells were harvested by scraping and then centrifuged at 500×*g* for 3 min at 4 °C. The supernatant was discarded and the pellet was resuspended in 500 µL of extraction buffer (220 mM mannitol, 70 mM sucrose, 10 mM HEPES (pH 7.5), 1 mM EGTA) with 1 × Complete protease inhibitor cocktail (F. Hoffmann-La Roche Ltd, REF 11697498001). Subsequently, cells were homogenized by repeated pipetting (homogenate fraction). The homogenate was centrifuged at 900×*g* for 5 min to remove nuclei and unbroken cells. The supernatant was transferred to a new tube, and the previous passage was repeated until no visible pellet was observed. The resulting supernatant was then centrifuged at 11,000×*g* for 5 min to pellet the mitochondrial fraction. The supernatant (cytosolic fraction) was collected and stored for downstream analyses, and the mitochondrial pellet was resuspended in extraction buffer. A final concentration of 1% Triton X-100 was added to the three fractions obtained before protein quantification by Bradford assay (Bio-Rad DC Protein Assay 5000112, Hercules, US).

Enzymatic activity assays

The activity of recombinant WT and p.Gly176Arg variant was measured spectroscopically at 340 nm as the NADH formed in the reaction ($\varepsilon_M = 6220\ M^{-1}\ cm^{-1}$) following the addition of an enzymatic sample of 10 nM for WT (concentration for activity assays is always referred to the tetramer since it is the functionally active species) or up to 10 µM for p.Gly176Arg to a total of 0.35 mL of 10 µM SSA and 500 µM NAD^+ in 100 mM potassium phosphate buffer, 10 mM BME, pH 8. SSADH enzyme activity in cell extracts, or cytosolic or mitochondrial extracts was determined by the same absorbance assay with the following modifications. Either total soluble lysates, or cytosolic or mitochondrial lysates (10 µL) were pipetted in duplicates into a flat-bottom 96-well plate and incubated for 1 h at 37 °C with 190 µL of an enzyme reaction mix containing 50 mM TRIS, 150 mM KCl, 1 mM DTT, 0,02% BSA, 250 µM SSA, and 1 mM NAD^+. The SSADH-mediated reduction of NAD^+ to NADH was measured as an increase in absorbance at 340 nm with a TECAN Infinite 200 Microplate Reader (Tecan Group, Männedorf, Switzerland). To evaluate the activity of other NAD^+-reducing enzymes, the baseline values of samples incubated with a reaction mix without substrates were subtracted.

Spectroscopic analyses

All spectroscopic measurements were carried out at 25 °C in 100 mM potassium phosphate buffer, pH 8, unless otherwise stated. Absorbance spectra were recorded with a Jasco V-550 spectrophotometer (Jasco Europe S.R.L., Milano, Italy), whereas intrinsic fluorescence emission analyses were carried out in a Jasco FP-750 spectrofluorimeter (Jasco Europe S.R.L) at 0.1 mg/mL SSADH, with 5 nm excitation and emission bandwidths upon excitation at 295 nm. Circular dichroism (CD) spectra were acquired in a Jasco J-710 spectropolarimeter (Jasco Europe S.R.L) at a scan speed of 50 nm/min with 2 nm bandwidth, using 0.1 mg/mL and 1 mg/mL protein concentrations for the far UV (190–250 nm) and near UV/visible (250–500 nm) range, respectively. Thermal denaturation was performed by monitoring the CD signal at 222 nm of 0.1 mg/mL SSADH species on a 25–90 °C linear gradient with a temperature slope of 1.5 °C /min.

Dynamic light scattering (DLS) analyses

DLS measurements were obtained on a Zetasizer Nano ZS instrument (Malvern), using disposable ZEN0112 polystyrene cuvettes. Settings used for particle size measurements were as follows: solvent refractive index 1.330, viscosity 0.8872 cP, protein refractive index 1.450, protein absorption 0.001, temperature 25°C, equilibration 2 min, measurement angle 173, backscatter, analysis model multiple narrow modes. Samples were prepared at 3–4 µM protein concentration in 100 mM potassium phosphate buffer, pH 8. All samples were filtered using a 0.02 µm Anotop 10 filter (Whatman). Data on particle size and of mean count rate are reported as mean ± SEM of at least 40 measurements, each one consisting of 12–18 repetitions. Mean count rate was recorded at 25 °C, and the trace is representative of multiple measurements.

Size exclusion chromatography (SEC) analyses

The determination of the oligomeric size was carried out in 100 mM potassium phosphate buffer and 150 mM NaCl, 10 mM BME, pH 8. Different concentrations (from 0.1 to 4.5 mg/mL) of recombinant WT and p.Gly176Arg SSADH were loaded into a Superdex 200 (10/300) column (GE Healthcare, Boston, MA, USA) coupled to an ÄKTA Pure system (GE Healthcare) with a 280 nm absorbance signal detector. The molecular weight was determined by fitting to the appropriate calibration curve.

Measurement of the equilibrium dissociation constant, K_d, for NAD^+

The equilibrium dissociation constant, K_d, for NAD^+ was calculated by incubating 0.1 µM (monomer concentration) WT and p.Gly176Arg variant with different concentrations of NAD^+ (from 0.5 to 100 µM) and plotting the change in the intrinsic fluorescence emission (at 335 nm), following excitation of the enzyme at 280 nm, as a function of NAD^+ concentration and fitting it to the following equation:

$$Y = \frac{Y_{max} \cdot x}{K_d + x}$$

where Y refers to the change in intrinsic fluorescence at each NAD^+ concentration (independent variable *x*), Ymax refers to the maximal change in the intrinsic fluorescence at the saturating NAD^+ concentration.

Western Blotting (WB)

Protein lysates and pellets (15 µg) were separated on a 12% SDS-PAGE under reducing conditions, followed by transfer to a nitrocellulose membrane. After blocking the membrane with 5% milk powder (Roth, Karlsruhe, Germany) in TBST, the membrane was hybridized with one of the following primary antibodies: anti-SSADH (1:2000, SantaCruz sc-390754), anti-vinculin (1:2000, ABclonal Technology, Woburn, MA, USA), anti-TOM20 (1:2000, ABclonal Technology, Woburn, MA, USA), anti-Flag-tag (1:2000, ABclonal Technology, Woburn, MA, USA), and anti-actin (1:2000, cat. ab-8245, Abcam) as loading control. Thereafter, the membrane was incubated with secondary antibodies anti-mouse (1:2000, Dako, Gostrup, Denmark) or anti-rabbit (1:5000, ABclonal Technology, Woburn, MA, USA). Protein detection was performed using an Enhanced Chemiluminescence kit (SuperSignal™ West Femto/Pico Chemiluminescent Substrate, Thermo Fisher Scientific). The signals were detected with ChemiDoc MP (Bio-Rad). All images were acquired employing the optimal resolution settings of the Bio-Rad proprietary software. ImageJ was used for the densitometric analysis of WB bands. Each SSADH signal was normalized to the corresponding loading control (actin signal) for the graphical representation of the densitometric analysis.

Chemical chaperons

ALDH5A1 knockout HEK-293 T cells were seeded onto 6-well culture plates, transfected with WT or p.Pro234Ser variant SSADH, and the next day treated with 10 mM betaine (Selleckchem, Cologne, Germany), 0.5 mM NAD^+ (Sigma-Aldrich, Taufkirchen, Germany), or a combination of both. After 48 h, the cells were harvested and lysed as reported above and protein expression was evaluated by western blot.

Statistical analysis

Statistical analyses and data representations were performed using GraphPad Prism (GraphPad Software, LLC).

Results

The clinical and metabolic features of two SSADH deficiency patients

The first patient was diagnosed with SSADH deficiency at 5 years of age as part of an investigation of delayed developmental milestones. Diagnosis relied on whole-exome sequencing (WES), which revealed that the patient was a functional hemizygote harboring the c.526G > A variant (p.Gly176Arg) on one allele and a null allele[23].

Early developmental milestones were mildly delayed, including head control (6 months), independent sitting (9 months), and unaided walking (15 months). However, gross motor skills subsequently normalized, with Gross Motor Function Classification System (GMFCS) and Manual Ability Classification System (MACS) levels of 0 on formal assessment. Babbling began at 9 months, while first words emerged around 2 years of age. Receptive language was preserved, although mild expressive language difficulties persisted. He did not meet criteria for autism spectrum disorder or attention-deficit/hyperactivity disorder, though parents reported subtle challenges with peer relationships and mild inattention. Sleep difficulties were noted, primarily characterized by bedtime resistance, reduced sleep duration, and parasomnias.

On bedside assessment using the SSADH deficiency-specific, validated Clinical Severity Score (CSS)[22], he achieved a score in the higher range, reflecting relatively better functioning than with other scoring systems. He demonstrated only mild intellectual disability, intact receptive communication, and absence of significant motor impairment. Notably, he did not exhibit dystonia, ataxia, or dyskinesia, nor psychiatric features commonly associated with SSADH deficiency, including obsessive–compulsive disorder symptoms. Other behavioral problems, such as aggression, were also not reported. He had no history of seizures, and both electroencephalogram and brain magnetic resonance imaging (MRI) were normal. At 5.5 years of age, plasma GABA measured 3.65 µM/L and GHB 667.0 µM/L, values considered to be in the higher range within the SSADH deficiency population[8].

The second patient is a 6-year-old female, born at term following an uneventful pregnancy to non-consanguineous parents. Initial developmental milestones were attained within normal limits: the patient regularly achieved independent sitting and produced her first words at 9 months of age. At approximately 12 months, a global deceleration in her developmental trajectory was observed. Independent ambulation was acquired with delay at 23 months accompanied by clumsiness and impaired gross and fine motor coordination. A key feature of the delayed developmental trajectory was a significant impairment of expressive language. Following the initial acquisition of single words, the patient experienced a period of language development arrest. By the age of 4.5 years, her expressive vocabulary was limited to approximately 10 isolated words with no evidence of word-pairing.

At the age of 4.5 years, an extensive diagnostic workup was conducted. Brain MRI revealed symmetrical T2/FLAIR hyperintensities involving prominent hyperintensities within the bilateral globus pallidus (Fig. 2A) and the bilateral dentate nuclei (Fig. 2B). Additionally, developmental venous anomalies (DVAs) with transparenchymal courses were identified in the right parietal region, right cerebellar lobe, and right frontal periventricular region. The bilateral, symmetrical signal alterations in the dentate nuclei and pallidum strongly suggested an inborn error of metabolism. Electrophysiological studies included an electroencephalogram, which revealed partially organized background activity interspersed with diffuse polyspike-and-wave discharges, clinically corresponding to episodes of eyelid myoclonia.

Given the suspicion of SSADH deficiency, urinary organic acid analysis was performed and confirmed increased excretion of GHB and 4,5-dihydroxyhexanoic acid.

Molecular confirmation was obtained through Next-Generation Sequencing (NGS) using a targeted gene panel. The analysis identified a paternal missense, pathogenic (ACMG 5) variant, c.700C > T (p.Pro234Ser), in exon 4 of *ALDH5A1* gene, and a maternal heterozygous deletion of approximately 400 kb encompassing the entire *ALDH5A1* locus. The deletion was subsequently confirmed by array-based comparative genomic hybridization (array-CGH) analysis. Thus, the only possible functional SSADH protein, that could theoretically be assembled from the synthesized individual polypeptide chains, is the p.Pro234Ser homotetramer.

The patient's clinical status has remained stable over time. At the most recent follow-up (age 6 years), neurological examination revealed an intention tremor and persistent impairment in fine and gross motor skills. Her expressive language deficit remains the most prominent feature, contrasting with her better-preserved receptive language; she communicates her needs primarily through non-verbal means (e.g., pointing).

Seizures remain stable, as the patient experiences daily eyelid myoclonia. Despite trials of multiple anti-seizure medications, including lamotrigine, levetiracetam, clobazam, rufinamide, zonisamide, topiramate, and ethosuximide, only valproic acid has provided a modest reduction in seizure frequency to date.

In silico analysis of the predicted structural impact of Gly176Arg and Pro234Ser substitutions

A deeper examination of the structural segment (amino acids 174–195) of the oligomeric domain in the SSADH tetramer (Fig. 3A) shows that Gly176 is located in an antiparallel β-sheet that mediates the interaction between two opposed monomers in the tetramer through a hydrophobic cluster composed of Ile178, Leu189, Val90 and Leu191, and their counterparts in the other monomer. In particular, the carbonyl group of Gly176 (black circle)

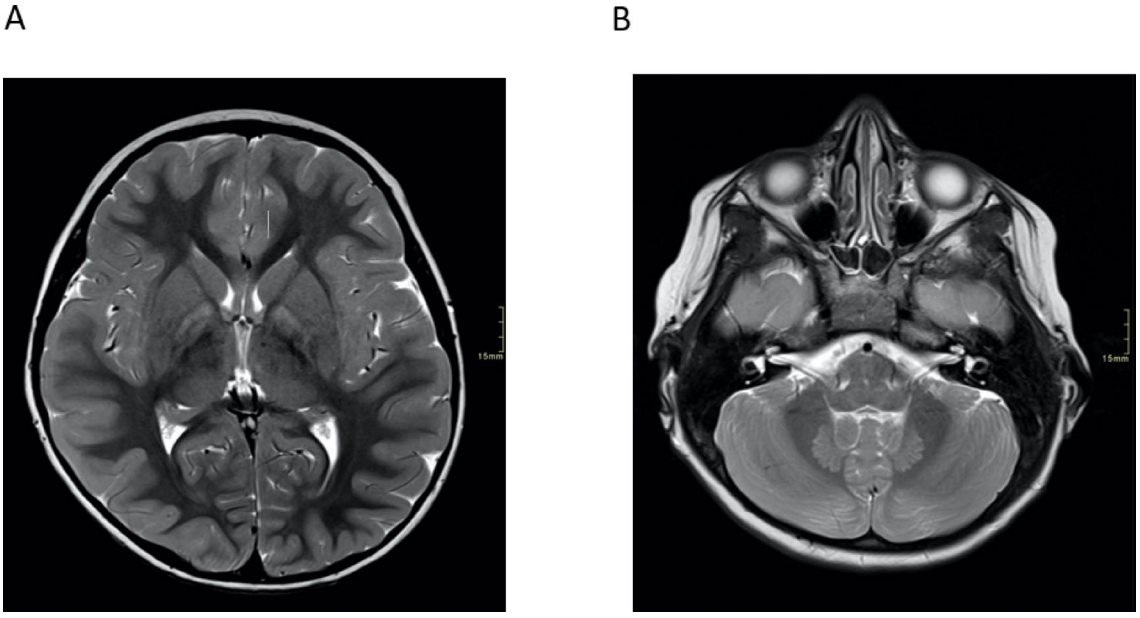


Fig. 2. Brain MRI of patient with p.Pro234Ser variant. Brain MRI performed at the age of 4.5 years. Axial T2-weighted images show marked bilateral symmetric hyperintensity of the globus pallidus (**A**) and dentate nuclei (**B**).

contacts the amidic nitrogen of Ile178 and the carbonyl of Asp177 of the same monomer, which is in contact with the same structural element on the neighboring monomer (Fig. 3B). The substitution of Gly176 with Arg alters the polarity and, due to its bulky side chain, determines steric clashes with the hydrophobic cluster composed by Ile178, Leu189, Val 190 and Leu191 in the monomer, and their counterparts in the other monomer involved in the interaction (Fig. 3B).

Pro234 is located at the beginning of a short, partially exposed alpha-helix in the NAD^+ binding domain. The loop preceding Pro234 seems to be maintained in position by the residue itself and by Pro229. Additionally, Pro234 is inserted in a highly hydrophobic pocket composed of three proline residues, two phenylalanine residues, and three valine residues, one alanine residue and two leucine residues (Fig. 3C). The substitution to Ser may both affect the stability of the loop to which residue 234 belongs, and alter the hydrophobicity of this area causing a repulsion of a beta-hairpin structure (amino acids 75–91) located just above the residue (Fig. 3C), and inducing the disassembly of the external surface formed by the SSADH N-terminal chain.

To further investigate the structural consequences of the identified variants, AlphaFold models of the tetrameric p.Gly176Arg and p.Pro234Ser proteins were generated and compared with the WT structure. No major alterations in the overall quaternary architecture were observed for either variant, suggesting preservation of the global fold (Fig. 3D). Nevertheless, a subtle reduction in local secondary-structure organization was noted in the region surrounding residue 234 in the p.Pro234Ser model. Because static structural models may not fully capture the energetic consequences of amino acid substitutions, additional stability analyses were performed using three independent computational approaches: FoldX, DynaMut2, and DUET. Despite methodological differences, all predictors consistently classified both variants as destabilizing.

FoldX analysis of the tetrameric assembly predicted a marked destabilizing effect for p.Gly176Arg ($\Delta\Delta G = +33.34 \pm 1.28$ kcal/mol), substantially greater than that observed for p.Pro234Ser ($\Delta\Delta G = +12.10 \pm 0.68$ kcal/mol) (Table 1). Independent predictors yielded smaller absolute values but reached the same qualitative conclusion, with DynaMut2 and DUET predicting destabilization for both variants (Table 1).

Collectively, these findings indicate that neither variant is expected to dramatically alter the overall SSADH tetrameric fold, but both are predicted to reduce protein stability. The effect appears particularly pronounced for p.Gly176Arg, suggesting a stronger perturbation of the energetic stability of the tetrameric assembly, even if also the Pro234-to-Ser substitution triggers structural local disruption.

The pathogenicity of Gly176-to-Arg substitution is related to an instability due to an altered tetrameric shape

Recombinant p.Gly176Arg variant was cloned, expressed and purified as reported in the Materials and Methods section. Both the yield (5% of WT) and the activity (0.02% of WT) were extremely low. The activity value is in agreement with that (less than 1%) previously reported for pathogenic SSADH deficiency variants following expression in HEK-293 T cells[13]. To understand the structural basis for the loss-of-function, we characterized the spectroscopic properties of the variant with respect to the WT species. The far UV CD spectra showed no gross modification in secondary structure content (Fig. 4A), although the melting temperature (T_m) at 222 nm for the variant was lower than that of the WT both in the absence and in the presence of NAD^+ (Table 2).

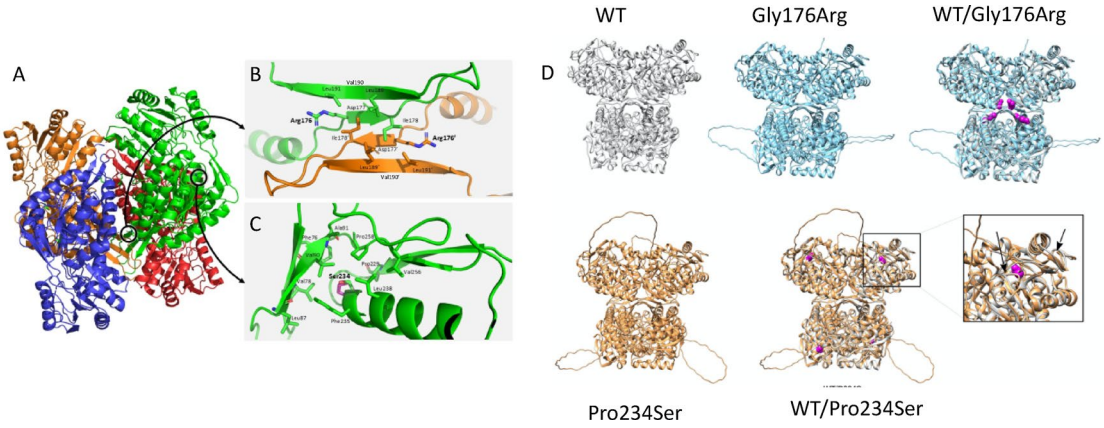


Fig. 3. In silico effects of the p.Gly176Arg and p.Pro234Ser substitutions. (**A**) The tetrameric structure of human SSADH (PDB 2W8O) is composed of a dimer of dimers, in which each monomer is represented with a different colour: first dimer green and red, second dimer orange and blue. The substituted Gly176Arg and Pro234Ser are circled on the green monomer. (**B**) Magnification of the microenvironment of Arg176 (the superimposed WT side chain of Gly176 is not visible). The hydrophobic cluster here represented is formed by part of the oligomerization domains (residues 172–194) of both the green and the orange monomers. The images presented here were created by PyMOL Molecular Graphics System (Version 3.1.6.1, Schrödinger, LLC). (**C**) Magnification of the microenvironment of Ser234 (superimposed in magenta the WT residue, Pro234). The loop, in which Ser234 and Pro229 are localised, finds in a hydrophobic cluster generated by residues (e.g. Phe76, Val78, Leu87, Val90, Ala91, Phe235, Leu238, Val256, and Pro258) of a beta-hairpin structure (residues 75–91). (**D**) Structural comparison of AlphaFold-predicted tetrameric WT and variants SSADH. AlphaFold models of the tetrameric p.Gly176Arg (top panels) and p.Pro234Ser (bottom panels) variants were generated and superimposed onto the WT SSADH structure. The WT structure is shown in grey, p.Gly176Arg in light blue, and p.Pro234Ser in orange. Substituted residues are highlighted as magenta spheres. The subtle rearrangement in the region surrounding residue 234 is shown in the boxed area. The images were created by PyMOL Molecular Graphics System (Version 3.1.6.1, Schrödinger).

Variant	FoldX (tetramer) ΔΔG (kcal/mol)	DynaMut2 ΔΔG (kcal/mol)	DUET ΔΔG (kcal/mol)	Overall prediction
p.Gly176Arg	+33.34 ± 1.28	−3.15	−1.22	Destabilizing
p.Pro234Ser	+12.10 ± 0.68	−0.95	−2.98	Destabilizing

Table 1. Predicted stability effects of the p.Gly176Arg and p.Pro234Ser SSADH variants using independent computational approaches.

Interestingly and differently from the WT, the variant was less stable and seemed unsensitive to the presence of the cofactor, that stabilizes the WT[21]. This raised the question regarding the ability of the variant to bind NAD^+ and the possibility that its loss-of-function could be due to an impairment in cofactor binding. The near UV–visible CD spectra of p.Gly176Arg were nearly similar in the region of aromatic amino acids both in the absence or presence of NAD^+, underlying no distinct folding damage (Fig. 4B). However, the dichroic signal in the visible region attributed to cofactor binding to the WT (visible also in absorbance spectra (inset of Fig. 4B)) was faint in the variant, suggesting both decrease in affinity or a different chiral environment (Fig. 4B). As the K_d for NAD^+ was nearly identical between the two species (Fig. 4C and Table 2), a decrease in NAD^+ affinity can be ruled out, even though the total amount of enzyme-cofactor (B_{max}) complex in the variant was 70% that of the WT (Fig. S1). This decrease as well as the 2 nm blue-shift in emission wavelength and a relative value of intrinsic fluorescence of the variant (about 10% higher than WT) can be interpreted as a slight modification of the NAD^+ binding site.

To check if p.Gly176Arg oligomerization is affected, we carried out SEC analyses (Fig. 4D) and compared them with the WT (Fig. S2). Unexpectedly, at least in the range of the chosen concentrations, the obtained molecular weight of the variant corresponds to a tetramer just like the WT. Indeed, DLS analyses of WT and p.Gly176Arg SSADH show a statistically significant increase of the hydrodynamic diameter (12.0 ± 0.1 nm for the variant with respect to 11.6 ± 0.1 for WT) (Fig. 4E), suggesting a loose and less compact tetramer shape for the variant that leads to instability and higher propensity to aggregate with respect to the WT (Fig. 4F).

The p.Pro234Ser variant prevents maturation of SSADH

Cloning, expression and purification of the p.Pro234Ser variant in bacteria resulted in a faint fraction of an insoluble 54 kDa species, preventing any other investigation with the recombinant species (Fig. S3). The artificial substitution p.Pro234Ala, performed to preserve the chemical nature of residue 234, gave the same results (data not shown) preventing us to obtain the recombinant protein variant.

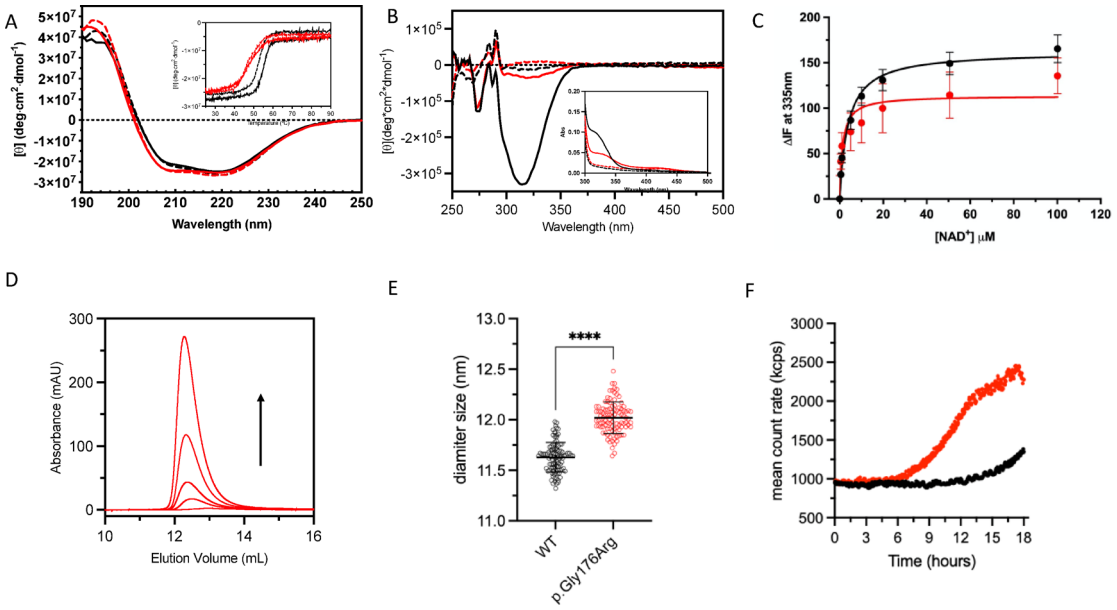


Fig. 4. Spectroscopic and chromatographic features of p.Gly176Arg. All spectra were collected in 100 mM potassium phosphate buffer, 10 mM BME at pH 8 at 25° C. Color code is black for WT and red for p.Gly176Arg in all panels. (**A**) Far UV CD spectra of 2 μM monomer protein concentration in the absence (dashed line) or presence of 100 μM NAD^+ (solid line); inset, thermal denaturation of the protein species under the same conditions. (**B**) Near UV–visible spectra of 18 μM monomer protein concentration in the absence (dashed line) or presence (solid line) of 200 μM NAD^+; inset, absorbance spectra of the protein species under the same conditions. (**C**) Plot of the change of intrinsic emission fluorescence at 335 nm (following excitation at 280 nm) of 0.1 μM monomer protein concentration in the presence of different concentrations of NAD^+ (i.e., 0, 0.5, 1, 5, 10, 20, 50, 100 μM). Points are mean values ± SD of two replicates for each protein and were fitted (solid line) to a hyperbola equation as described in the Materials and Methods section. (**D**) SEC analysis of p.Gly176Arg carried out at 25 °C in 100 mM potassium phosphate buffer, 0.15 M NaCl, 10 mM BME, pH 8.0 as mobile phase at different protein concentrations (0.1 mg mL^{-1}, 0.45 mg mL^{-1}, 0.90 mg mL^{-1}, 2.25 mg mL^{-1}, 4.50 mg mL^{-1}). The arrow indicates the increase in concentration. (**E**) Hydrodynamic diameters determined by DLS. Particle sizes values derive from multiple runs of three independent experiments and are reported as mean ± SEM. Statistical differences were determined with unpaired t-test analysis. $^{****}P < 0.0001$ in comparison to the WT. (**F**) Mean count rate of WT and p.Gly176Arg measured during the incubation time. The trace represents the values of the mean count rate of each repetitive measurement at the same time.

	T_m (°C) no NAD^+	T_m (°C) with NAD^+	K_d NAD^+ (μM)	Y_{max} ($\Delta IF_{335\,nm}$)
WT	52.72 ± 0.02	55.07 ± 0.03	3.8 ± 0.1	162 ± 20
p.Gly176Arg	46.75 ± 0.05	47.92 ± 0.07	1.6 ± 0.7	115 ± 31

Table 2. Determination of the Tm for WT and p.Gly176Arg SSADH in the absence or presence of 100 μM NAD^+ and evaluation of the K_d of the cofactor for both species.

The expression of p.Pro234Ser variant was then carried out in KO HEK-293 T cells resulting in a partitioning between the insoluble pellet fraction and the soluble fraction (Figs. 5A, S4). Even if also the WT enzyme is present in the insoluble pellet, the amount of the variant is higher, underlying the tendency to be insoluble, as in bacterial cells. Interestingly, the soluble fraction shows a predominance of the immature SSADH form (MTS not cleaved (Fig. 5B)) for the variant, whereas only a faint band for the mature form (about 4% of the immature one) was observed by WB analyses. Instead, the WT shows a ratio of about 50% of the immature to mature forms in the soluble fraction.

SSADH activity was measured in crude cell lysates from KO HEK-293 T cells transiently transfected with either WT or p.Pro234Ser constructs. Transient expression of the WT protein restored SSADH activity to 59 ± 9 nmol/min/mg, while the KO HEK-293 T activity is 0.58 ± 0.09 nmol/min/mg. Instead, transient transfection of KO HEK-293 T cells with the p.Pro234Ser variant resulted in an activity of 0.62 ± 0.03 nmol/min/mg, corresponding to approximately 1% of WT-transfected cells and indistinguishable from that observed in KO HEK-293 T cells. These findings indicate that the p.Pro234Ser variant lacks detectable SSADH activity (Fig. 5C).

The variant compartmentalizes between cytosol and mitochondria, as the WT, with a stronger prevalence of the immature form for p.Pro234Ser than the WT (Figs. 5D and E, S5, S6 and S7). In detail, while in the cytosol the total intensity of the signals is nearly identical for WT and p.Pro234Ser, with a partitioning between

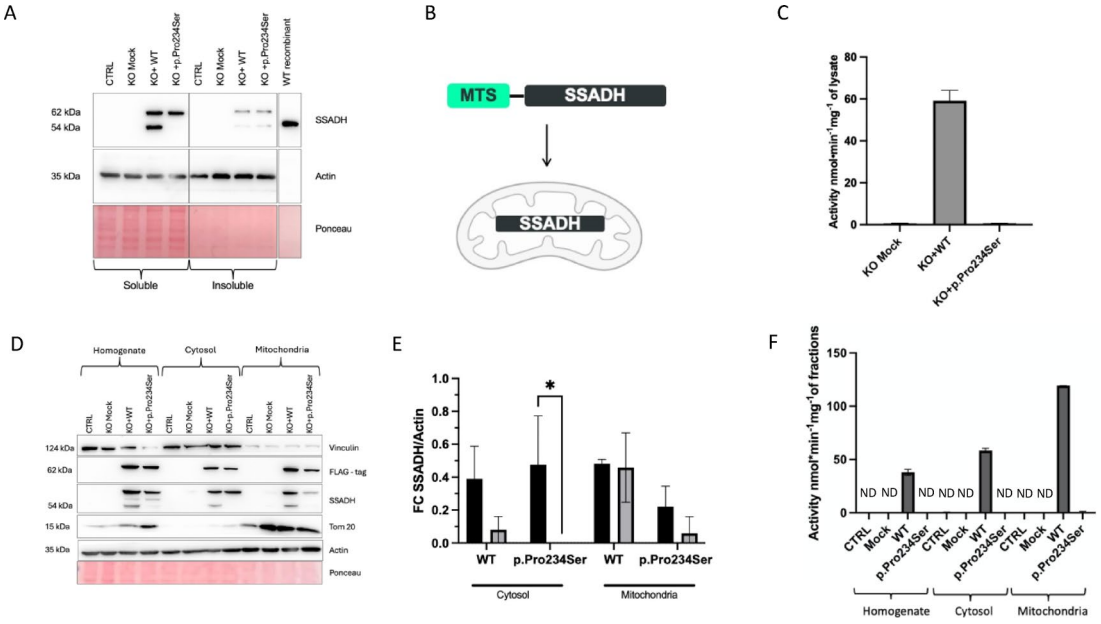


Fig. 5. Expression, localization and activity of WT and p.Pro234Ser SSADH. (**A**) Expression of SSADH in the soluble and insoluble fraction of crude extracts obtained from non-transfected HEK-293T cells as control (CTRL) and transiently transfected HEK-293T KO cells with empty plasmid (Mock), SSADH WT (KO + WT), SSADH p.Pro234Ser (KO + p.Pro234Ser). Recombinant WT SSADH was employed as a mature SSADH control, and actin as loading control. The image was derived from a single membrane. Original blots are reported in Supplementary Fig. S4. (**B**) Graphical representation of immature SSADH and its transport into mitochondrial matrix where it folds into SSADH mature form. (**C**) Activity of lysates of KO HEK-293T cells transiently transfected with WT or p.Pro234Ser SSADH incubated for 1h at 37°C with 190 µL of an enzyme reaction mix containing 50 mM TRIS, 150 mM KCl, 1 mM DTT, 0,02% BSA, 250 µM SSA, and 1 mM NAD^+. The values are reported as the mean of two independent experiments ± SD. (**D**) Expression of SSADH in the crude extract, and in the cytosolic and mitochondrial fractions of cell lysates from non-transfected HEK-293T cells as control (CTRL) and transiently transfected HEK-293T KO cells with empty plasmid (Mock), SSADH WT (KO + WT), SSADH p.Pro234Ser (KO + p.Pro234Ser). Vinculin, TOM 20, actin and flag-tag were employed as internal controls to verify the isolation efficiency of the cytosolic and mitochondrial fractions and the loading, respectively. This is one representative WB of three independent experiments. Original blots of the experiment are reported in Supplementary Figs. S5, S6 and S7. (**E**) Fold-change (FC) of the densitometric area of mature (light grey) and immature (black) SSADH bands in cytosolic and mitochondrial compartments. WT and p.Pro234Ser SSADH bands in the cytosol and in the mitochondria of the WB of the three replicates (panel (D) and Figs. S5, S6 and S7) were quantified by determining the band density normalized to the corresponding loading control (actin signal) with the ImageJ software. Statistical differences were determined for the three replicates with two-way ANOVA. The mean ± SD was shown; $*p < 0.5$. (**F**) Residual SSADH activity in the crude extract, and in the cytosolic and mitochondrial fractions of cell lysates from non-transfected HEK-293T cells as control (CTRL) and transiently transfected HEK-293T KO cells SSADH WT (KO + WT), SSADH p.Pro234Ser (KO + p.Pro234Ser). ND, not detectable.

immature (83%) and mature (17%) forms for the WT, the variant is significantly present as immature form (100%). In the WT mitochondrial fraction, the equilibrium between immature (52%)/mature (48%) form is lower than in the cytosol, with an enrichment of the active mature SSADH. For p.Pro234Ser proportionally less SSADH is found in the mitochondrial fraction (46% of the WT), with a relative persistence of the immature (79%) with respect to mature (21%) form. Therefore, data suggest a pathogenic defect in some steps associated with the maturation process (Fig. 5B).

Activity measurements on homogenates and the purified cytosolic and mitochondrial fractions show a progressive enrichment in SSADH activity for the WT (from 38 ± 3 nmol/min/mg in the homogenate, to 58 ± 2 nmol/min/mg in the cytosol, to 116.3 ± 0.1 nmol/min/mg in the mitochondrial fraction), as expected by the relative increase of the mature to immature form from cytosol to mitochondria. Instead, the p.Pro234Ser variant remained nearly inactive (from nearly zero nmol/min/mg in both the homogenate and the cytosol, to 0.87 ± 0.6 nmol/min/mg in the mitochondrial fraction) and was present predominantly in the immature form (Fig. 5F). It can thus be suggested that the variant maturation is impaired, possibly due to its intrinsic instability rather than a defect in the maturation apparatus, since a small fraction of p.Pro234Ser is able to gain a mature, but still basically inactive, form, possibly due to the misfolding defect triggered by the amino acid substitution. The treatments with the chemical chaperone betaine and the cofactor NAD^+ were ineffective with both WT and p.Pro234Ser variant, which, differently from the WT, predominantly remains in the immature state in the soluble fraction (Figs. 6, S8).

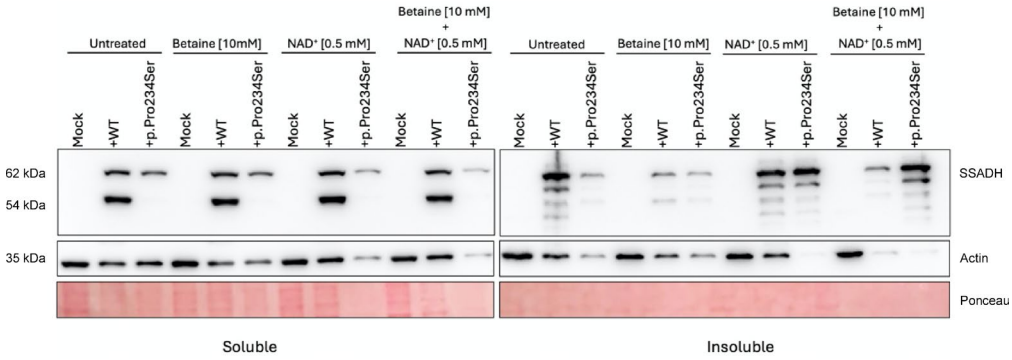


Fig. 6. SSADH expression following treatment with molecular chaperones. The expression levels of SSADH were evaluated by WB analysis both in the soluble and insoluble fractions of transiently transfected HEK-293T KO cells with empty plasmid (Mock), SSADH WT (+WT), SSADH p.Pro234Ser (+p.Pro234Ser). Cells were treated with 10 mM of betaine or 0.5 mM of NAD^+, or the combination of both. As control samples (untreated), cells were transiently transfected and maintained in the same conditions without treatment. Actin was employed ad loading control. Original blots are reported in Supplementary Fig. S8.

Discussion

We developed a multi-approach in-depth characterization of two pathogenic SSADH deficiency variants belonging to patients that can theoretically express only one type of polypeptide SSADH chain from their known genotypes.

The first variant, p.Gly176Arg[13,17], was already reported to be almost inactive in in vitro cell transfection experiments (< 1% residual activity)[13]. Since Gly176 belongs to a stretch (amino acids 174–195) of the oligomerization domain, the reason for the loss-of-function was attributed to a failure for SSADH to reach a competent tetrameric structure[19,23]. A different variant of the same residue p.Gly176Glu, identified in a Chinese child in compound heterozygosis[31], was described almost inactive (1% residual activity)[16], too, underscoring how profoundly the substitution of a glycine in that position can impact activity.

The recombinant purified variant is largely affected (activity 0.02% that of the purified WT) in agreement with the data collected by transient transfection in mammalian cells[13]. Here we demonstrate that its loss-of-function is not due to a defect in acquiring an oligomeric structure, but to a relaxed, expanded size of the p.Gly176Arg homotetramer. When compared to the WT, the p.Gly176Arg protein population shows a prevalence of species with increased hydrodynamic diameter (Fig. 4E). This larger tetramer is unstable since it tends to aggregate at a faster rate than the WT (Fig. 4F). Its instability is also supported by the bioinformatic analyses. The altered tetrameric shape, but not its affinity, seems to affect the formation of the stabilizing enzyme-NAD^+ complex[21], revealing that p.Gly176Arg variant would still be able to bind the cofactor (Fig. 4A-C) and possibly even to perform catalysis if the stretching process and the related aggregation drift could be blocked. Notably, the genotype-to-phenotype correlations predicted that p.Gly176Arg, either as a single homotetramer or as a heterotetramer in combination with multiple homo and heterotetramers (as in compound heterozygosis), is associated with the mildest clinical severity[23]. Effectively, the patient described has a mild phenotype. This can be explained by the role played by chaperones in a cellular context in correcting misfolding, as well as by the presence of other tetrameric species (in compound heterozygous patients) that mitigate the effect of this variant. The knowledge of the molecular basis of the structural and functional impact, achieved by combining in silico and in solution experiments, can be helpful to orient to therapeutic choice.

The patient harboring the p.Pro234Ser variant in functionally hemizygosis presents instead a moderate clinical phenotype. The most important finding of the p.Pro234Ser variant is its inherent instability, possibly due to the fact that most of the variant population does not reach maturation. Mitochondrial-targeted proteins are synthesized in the cytosol as completely or partially unfolded and then transferred to the mitochondrial matrix by a shared effort of the translocases complexes of the outer (TOM) and inner (TIM23) mitochondrial membrane complexes. The first one is an outer membrane protein complex that recognizes the mitochondrial targeting sequences and functions as a general gate for immature proteins into mitochondria. The second one is an inner membrane protein complex that allows the translocation of immature proteins into the mitochondrial matrix[32]. After the translocation into the mitochondrion, the immature protein is recognized by the mitochondrial-processing peptidase which proteolytically removes the targeting sequence and frees the protein that is then allowed to fold into the enzymatically mature and active form, often in the presence of a mitochondrial chaperones, such as mtHsp70. Up to date, it is not clear if SSADH folds directly into its final active form or if there is an intermediate stage in which the pro-peptide folds into a monomeric protein, four of which assemble in a quaternary structure. The full-length WT SSADH polypeptide chain is unable to fold into an active tetramer when expressed in bacteria, and resulted as an insoluble species recovered only in the pellet (Cesaro S. and Bertoldi M., unpublished results), mainly due to the absence of chaperones that are instead present in mammalian cells. Our results show that a small fraction of mature WT SSADH is present and active in the cytosolic fraction and is enriched in the mitochondria, as expected (Fig. 5C,D). Instead, for the p.Pro234Ser variant, the equilibrium between the immature and the mature form is strongly displaced towards

the immature one both in the cytosolic and mitochondrial fraction and no activity could be detected (Fig. 5C,D). However, a small amount of mature p.Pro234Ser species is indeed found (always visible in the insoluble fraction (Fig. 5A) and in the enriched mitochondrial fraction (Fig. 5D)). This would rule out a direct role of Pro234 in the maturation. Rather, its conversion to Ser produces a change of chemical environment and conformation, as also suggested by bioinformatic modeling, possibly leading to inability to fold. The accumulation of unfolded chains could function as a bottle neck and would prevent further maturation. Thus, the molecular basis for the loss-of-function of p.Pro234Ser consists of a misfolding defect leading to accumulation of the immature form. The failure of betaine and/or the NAD^+ cofactor to exert a chaperone effect to increase the expression or activity of both WT and p.Pro234Ser (Fig. 6) is similar to what already described for other SSADH variants[24], raising the question of the need of more targeted chaperones for SSADH.

Although the molecular analysis carried out here concerns a limited number of variants, and this could be an intrinsic limit of this study, it should be pointed out that SSADH deficiency is an ultrarare disease with only some hundreds of patients identified so far worldwide[4] and only few variants have been characterized in details, reporting the molecular basis for their the loss-of-function[24].

Interestingly, AlphaFold modelling and energetic stability predictions provided complementary rather than contradictory information. While AlphaFold suggested that both variants remain compatible with the native tetrameric architecture, FoldX, DynaMut2, and DUET consistently predicted reduced protein stability. These observations suggest that the pathogenic effects of p.Gly176Arg and p.Pro234Ser may arise from destabilization of the native structure rather than from gross alterations of the overall fold.

In conclusion, the combination of approaches obtained from in silico analyses, and recombinant protein characterization and expression in an appropriate cell model of two SSADH deficiency variants has contributed to the dissection of the molecular basis for the variant defects. These findings should orient SSADH deficiency research toward addressing the folding and the tetramer formation steps.

Values represent the mean FoldX ΔΔG obtained from five independent runs performed on the tetrameric assembly. Positive FoldX values and negative DynaMut2/DUET values indicate reduced protein stability. Although the absolute magnitudes differ among methods because of distinct scoring functions and structural contexts, all predictors consistently classified both variants as destabilizing. Positive FoldX ΔΔG values and negative DynaMut2/DUET ΔΔG values indicate destabilization relative to the WT protein.

Data availability

All data are available upon a reasonable request to the corresponding author.

Received: 18 April 2026; Accepted: 14 July 2026
Published online: 17 July 2026

References

1. Pearl, P. L. et al. Succinic semialdehyde dehydrogenase deficiency: Review of the natural history study. *J. Child Neurol.* **36**, 1153–1161. https://doi.org/10.1177/0883073820981262 (2021).
2. Malaspina, P. et al. Succinic semialdehyde dehydrogenase deficiency (SSADHD): Pathophysiological complexity and multifactorial trait associations in a rare monogenic disorder of GABA metabolism. *Neurochem. Int.* **99**, 72–84. https://doi.org/10.1016/j.neuint.2016.06.009 (2016).
3. Martin, K., McConnell, A. & Elsea, S. H. Assessing prevalence and carrier frequency of succinic semialdehyde dehydrogenase deficiency. *J. Child Neurol.* **36**, 1218–1222. https://doi.org/10.1177/08830738211018902 (2021).
4. Didiášová, M. et al. Succinic semialdehyde dehydrogenase deficiency: An update. *Cells* https://doi.org/10.3390/cells9020477 (2020).
5. Pearl, P. L. et al. Inherited disorders of gamma-aminobutyric acid metabolism and advances in ALDH5A1 mutation identification. *Dev. Med. Child Neurol.* **57**, 611–617. https://doi.org/10.1111/dmcn.12668 (2015).
6. Tokatly Latzer, I. et al. The presence and severity of epilepsy coincide with reduced gamma-aminobutyrate and cortical excitatory markers in succinic semialdehyde dehydrogenase deficiency. *Epilepsia* **64**, 1516–1526. https://doi.org/10.1111/epi.17592 (2023).
7. Tokatly Latzer, I. et al. Autism spectrum disorder and GABA levels in children with succinic semialdehyde dehydrogenase deficiency. *Dev. Med. Child Neurol.* https://doi.org/10.1111/dmcn.15659 (2023).
8. Tokatly Latzer, I. et al. Clinical and molecular outcomes from the 5-year natural history study of SSADH deficiency, a model metabolic neurodevelopmental disorder. *J. Neurodev. Disord.* **16**, 21. https://doi.org/10.1186/s11689-024-09538-9 (2024).
9. Tokatly Latzer, I. et al. The neuropsychological profile of SSADH deficiency, a neurotransmitter disorder of GABA metabolism. *Mol. Genet. Metab.* **144**, 109051. https://doi.org/10.1016/j.ymgme.2025.109051 (2025).
10. Tokatly Latzer, I. et al. Central dysmyelination in SSADH-deficient humans and mice. *Ann. Clin. Transl. Neurol.* **12**, 2193–2205. https://doi.org/10.1002/acn3.70148 (2025).
11. Gibson, K. M. et al. 4-Hydroxybutyric aciduria: Application of a fluorometric assay to the determination of succinic semialdehyde dehydrogenase activity in extracts of cultured human lymphoblasts. *Clin. Chim. Acta* **196**, 219–221. https://doi.org/10.1016/0009-8981(91)90076-o (1991).
12. Tokatly Latzer, I. et al. Consensus guidelines for the diagnosis and management of succinic semialdehyde dehydrogenase deficiency. *Mol. Genet. Metab.* **142**, 108363. https://doi.org/10.1016/j.ymgme.2024.108363 (2024).
13. Akaboshi, S. et al. Mutational spectrum of the succinate semialdehyde dehydrogenase (ALDH5A1) gene and functional analysis of 27 novel disease-causing mutations in patients with SSADH deficiency. *Hum. Mutat.* **22**, 442–450. https://doi.org/10.1002/humu.10288 (2003).
14. Blasi, P. et al. Structure of human succinic semialdehyde dehydrogenase gene: Identification of promoter region and alternatively processed isoforms. *Mol. Genet. Metab.* **76**, 348–362. https://doi.org/10.1016/s1096-7192(02)00105-1 (2002).
15. Menduti, G. et al. Succinic semialdehyde dehydrogenase deficiency: The combination of a novel ALDH5A1 gene mutation and a missense SNP strongly affects SSADH enzyme activity and stability. *Mol. Genet. Metab.* **124**, 210–215. https://doi.org/10.1016/j.ymgme.2018.05.006 (2018).
16. Pop, A. et al. Functional analysis of thirty-four suspected pathogenic missense variants in ALDH5A1 gene associated with succinic semialdehyde dehydrogenase deficiency. *Mol. Genet. Metab.* **130**, 172–178. https://doi.org/10.1016/j.ymgme.2020.04.004 (2020).
17. DiBacco, M. L. et al. Novel ALDH5A1 variants and genotype Phenotype correlation is SSADH deficiency. *Neurology* **95**, e2675–e2682. https://doi.org/10.1212/WNL.0000000000010730 (2020).

18. Leo, S. et al. SSADH deficiency in an Italian family: A novel ALDH5A1 gene mutation affecting the succinic semialdehyde substrate binding site. *Metab. Brain Dis.* **32**, 1383–1388. https://doi.org/10.1007/s11011-017-0058-5 (2017).
19. Kim, Y. G. et al. Redox-switch modulation of human SSADH by dynamic catalytic loop. *EMBO J.* **28**, 959–968. https://doi.org/10.1038/emboj.2009.40 (2009).
20. Kim, K. J. et al. Succinic semialdehyde dehydrogenase: Biochemical-molecular-clinical disease mechanisms, redox regulation, and functional significance. *Antioxid. Redox Signal.* **15**, 691–718. https://doi.org/10.1089/ars.2010.3470 (2011).
21. Cesaro, S. et al. A crucial active site network of titratable residues guides catalysis and NAD(+) binding in human succinic semialdehyde dehydrogenase. *Protein Sci.* **34**, e70024. https://doi.org/10.1002/pro.70024 (2025).
22. Tokatly Latzer, I., Roullet, J. B., Gibson, K. M. & Pearl, P. L. Establishment and validation of a clinical severity scoring system for succinic semialdehyde dehydrogenase deficiency. *J. Inherit. Metab. Dis.* **46**, 992–1003. https://doi.org/10.1002/jimd.12635 (2023).
23. Tokatly Latzer, I. et al. Phenotypic correlates of structural and functional protein impairments resultant from ALDH5A1 variants. *Hum. Genet.* **142**, 1755–1776. https://doi.org/10.1007/s00439-023-02613-6 (2023).
24. Didiasova, M. et al. Functional characterization of a spectrum of genetic variants in a family with succinic semialdehyde dehydrogenase deficiency. *Int. J. Mol. Sci.* https://doi.org/10.3390/ijms25105237 (2024).
25. Gibson, K. M. et al. The clinical phenotype of succinic semialdehyde dehydrogenase deficiency (4-hydroxybutyric aciduria): Case reports of 23 new patients. *Pediatrics* **99**, 567–574. https://doi.org/10.1542/peds.99.4.567 (1997).
26. Brennenstuhl, H. et al. Succinic semialdehyde dehydrogenase deficiency: In vitro and in silico characterization of a novel pathogenic missense variant and analysis of the mutational spectrum of ALDH5A1. *Int. J. Mol Sci.* https://doi.org/10.3390/ijms21228578 (2020).
27. Abramson, J. et al. Accurate structure prediction of biomolecular interactions with AlphaFold 3. *Nature* **630**, 493–500. https://doi.org/10.1038/s41586-024-07487-w (2024).
28. Delgado, J., Radusky, L. G., Cianferoni, D. & Serrano, L. FoldX 5.0: Working with RNA, small molecules and a new graphical interface. *Bioinformatics* **35**, 4168–4169. https://doi.org/10.1093/bioinformatics/btz184 (2019).
29. Rodrigues, C. H. M., Pires, D. E. V. & Ascher, D. B. DynaMut2: Assessing changes in stability and flexibility upon single and multiple point missense mutations. *Protein Sci.* **30**, 60–69. https://doi.org/10.1002/pro.3942 (2021).
30. Pires, D. E., Ascher, D. B. & Blundell, T. L. DUET: A server for predicting effects of mutations on protein stability using an integrated computational approach. *Nucl. Acids Res.* **42**, W314–W319. https://doi.org/10.1093/nar/gku411 (2014).
31. Jiang, S. Z. et al. Analysis of ALDH5A1 gene mutation in a Chinese Han family with succinic semialdehyde dehydrogenase deficiency. *Zhonghua Yi Xue Yi Chuan Xue Za Zhi* **30**, 389–393. https://doi.org/10.3760/cma.j.issn.1003-9406.2013.04.002 (2013).
32. Neupert, W. & Herrmann, J. M. Translocation of proteins into mitochondria. *Annu. Rev. Biochem.* **76**, 723–749. https://doi.org/10.1146/annurev.biochem.76.052705.163409 (2007).

Acknowledgements

We acknowledge the Centro Piattaforme Tecnologiche (CPT) of the University of Verona for the spectroscopic measurements.

Author contributions

GS and SC: Data collection, figures preparation, analysis and interpretation. Manuscript drafting.CACC: Data analysis and interpretation. Manuscript drafting.DT and FB: Clinical data collection. Manuscript draftingVB: Neuroradiological data collection. Manuscript draftingSP: Genetic analysis. Manuscript draftingITL, PLP: Data interpretation. Manuscript drafting.GB: DLS experiments, Data analysis and interpretation. Manuscript drafting. MD and RT: Analysis interpretation of cell collected data. Manuscript drafting.MB: Study conceptualization. Data interpretation. Manuscript writing.

Funding

This research was funded from SSADH-Defizit e.V. (grant 2019-01 and 2023-01) and from De Neu Asociación de Enfermedades de los Neurotrasmisores to MB.

Declarations

Competing interests

The authors declare no competing interests.

Ethics approval and informed consent

All procedures were in accordance with the 1964 Helsinki declaration and its later amendments or comparable ethical standards. Written informed consent for this work was obtained from the patient's parents or legal caregivers. We confirm that we have read the Journal's position on issues involved in ethical publication and affirm that this work is consistent with those guidelines. The Succinic Semialdehyde Dehydrogenase (SSADH) Deficiency Natural History Study (NHS) is approved by the Boston Children's Hospital Institutional Review Board (#P00029917). All participants in the SSADH Deficiency NHS reviewed and signed an informed consent form.

Additional information

Supplementary Information The online version contains supplementary material available at https://doi.org/10.1038/s41598-026-62784-w.

Correspondence and requests for materials should be addressed to M.B.

Reprints and permissions information is available at www.nature.com/reprints.

Publisher's note Springer Nature remains neutral with regard to jurisdictional claims in published maps and institutional affiliations.

Open Access This article is licensed under a Creative Commons Attribution-NonCommercial-NoDerivatives 4.0 International License, which permits any non-commercial use, sharing, distribution and reproduction in any medium or format, as long as you give appropriate credit to the original author(s) and the source, provide a link to the Creative Commons licence, and indicate if you modified the licensed material. You do not have permission under this licence to share adapted material derived from this article or parts of it. The images or other third party material in this article are included in the article's Creative Commons licence, unless indicated otherwise in a credit line to the material. If material is not included in the article's Creative Commons licence and your intended use is not permitted by statutory regulation or exceeds the permitted use, you will need to obtain permission directly from the copyright holder. To view a copy of this licence, visit http://creativecommons.org/licenses/by-nc-nd/4.0/.

© The Author(s) 2026